Preparation of $Eu(OH)_3$ and Eu_2O_3 Nanorods through a Simple Method

Xuefeng Yang, Guiling Ning,* and Yuan Lin
State Key Laboratory of Fine Chemicals and School of Chemical Engineering, Dalian University of Technology,
158 Zhongshan Road, Dalian 116012, P. R. China

(Received December 12, 2006; CL-061459; E-mail: ninggl@dlut.edu.cn)

$Eu(OH)_3$ and Eu_2O_3 nanorods were prepared by a facile hydrothermal procedure. The obtained hexagonal phase $Eu(OH)_3$ nanorods have diameter of about 50 nm and lengths ranging from 100 to 800 nm. Eu_2O_3 nanorods were obtained from $Eu(OH)_3$ by calcination. The Eu_2O_3 nanorods show a pure cubic phase and exhibit characteristic luminescence of Eu^{3+} ions at 616 nm.

Much attention has recently focused on one-dimensional (1D) nanostructures since the discovery of carbon nanotubes.[1] The unique physical and chemical properties of 1D nanotubes and nanorods have been well documented and proposed for a wide range of applications.[2] Up to now, some inorganic nanorods such as sulfides and oxides have been fabricated.[3] Rare earth (RE) oxides have been widely used as high-performance luminescent devices, magnets, catalysts, and other functional materials based on the electronic, optical, and chemical characteristics resulting from their 4f electrons.[4] Most of these advanced functions depend strongly on the compositions and structures, which are sensitive to the bonding states of rare earth atoms or ions. If rare earth oxides were fabricated in the form of a 1D nanostructure, they would hold promise as highly functionalized materials as a result of both shape-specific and quantum confinement effects. Among the RE elements, the luminescence of Eu^{3+} is particularly interesting because the major emission band is centered near 612 nm, which is one of the three primary colors. Therefore, Eu^{3+} ions have been studied intensively as a luminescent activator in many hosts lattices.[5] Eu_2O_3 is the most stable europium compound and one of the most important oxide phosphors, in which the ions hold typically a trivalent state. So far, nanostructured Eu_2O_3 crystals have been synthesized by means of laser evaporation,[6] sol–gel process,[7] and template approach.[8] However, to the best of our knowledge, only Pol et al. have reported the preparation of Eu_2O_3 nanorods by ultra-sound irradiation.[9] Here, we report a simple method for the direct growth of first $Eu(OH)_3$ nanorods by facile hydrothermal treatment of bulk Eu_2O_3 crystals.

In this experiment, 0.8 g of Eu_2O_3 powder (purity: 99.99%) was added to 50 mL of NaOH (10 M) solution and then poured into a 100-mL capacity Teflon-lined stainless autoclave. The autoclave was maintained at 150 °C for 24 h and then air-cooled to room temperature. The resulting products (0.91 g) were obtained by washing with water and drying at 60 °C for 2 h. As-made $Eu(OH)_3$ was calcined to produce Eu_2O_3 nanorods in air at 700 °C for 2 h, and the yield of Eu_2O_3 nanorods from raw bulk Eu_2O_3 is about 98.9%.

The morphology of starting bulk Eu_2O_3 was examined with transmission electron microscopy (TEM) taking on a Philips TECNAI G^2 s-twin microscope (Supporting Information 1).[13] The raw grains are irregular and include aggregation of small particles, and the average grain size is about 200 nm. In contrast to that of raw bulk Eu_2O_3, the TEM images of $Eu(OH)_3$ and Eu_2O_3 products were shown in Figure 1. It can be seen from Figure 1a, the $Eu(OH)_3$ products consist almost entirely of nanorods with the diameter of about 50 nm and lengths ranging from 100 to 800 nm. Dehydration of the $Eu(OH)_3$ nanorods leads to the formation of Eu_2O_3 nanorods (Figure 1b). Even after thermal treatment at 700 °C for 2 h, the frameworks of these nanorods are still maintained. These results demonstrate that $Eu(OH)_3$ and Eu_2O_3 nanotubes can be obtained by this simple method.

In order to further investigate the structure of obtained $Eu(OH)_3$ and Eu_2O_3 nanorods. The as-prepared samples were examined by X-ray diffraction (XRD) measurement on a Rigaku-DMax 2400 diffractometer equipped with graphite monochromatized Cu Kα ($\lambda = 1.5406$ Å). All of peaks of the XRD patterns in Figure 2a can be readily indexed to a hexagonal phase [space group: $P6_3/m$ (176)] of $Eu(OH)_3$ with lattice constants $a = 6.352$ Å, $c = 3.653$ Å (JCPDS 83-2305). Figure 2b shows that pure Eu_2O_3 phase was obtained by calcination of as-made $Eu(OH)_3$. All of the peaks are attributed to a pure cubic phase [space group: $I2_13$ (199)] of transformed Eu_2O_3 with lattice constants $a = 10.84$ Å (JCPDS 76-0154). Thermogravimetric ananlysis indicates that $Eu(OH)_3$ has converted completely to Eu_2O_3 by calcinations at 700 °C (Figure 3). The obtained thermogravimetric result is similar to the report of Pol et al.[9] It presents three stages of weight loss and the total weight loss of about 13%. The initial weight loss at the temperature of 100 °C results from desorption of water molecules from the surface of the nanorods. The second decomposition occurred at 300 °C, which is attributed to the conversion of $Eu(OH)_3$ to EuOOH. The last stage is due to the transformation of EuOOH to Eu_2O_3 at the temperature ranging from 400 to 700 °C.

The luminescent property of the Eu_2O_3 nanorods was characterized by a JASCO FP-6300 spectrofluorometer with an excitation wavelength of 396 nm, which is shown in Figure 4. The intense emission peak at 616 nm is due to the hypersensitive $^5D_0$–$^7F_2$ transition running using forced parity electric dipole

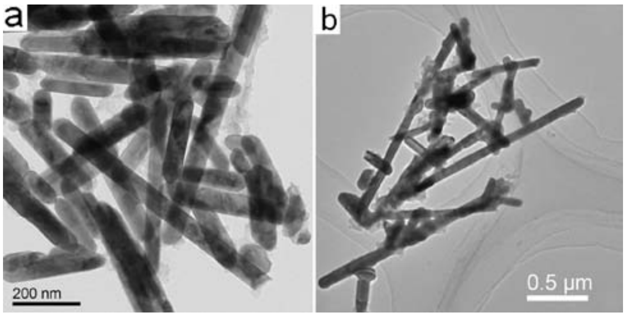

Figure 1. TEM images of (a) $Eu(OH)_3$ and (b) Eu_2O_3 nanorods.

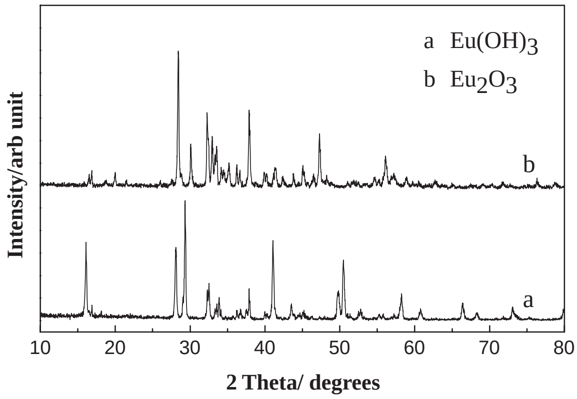

Figure 2. XRD patterns of the obtained $Eu(OH)_3$ and Eu_2O_3 nanorods.

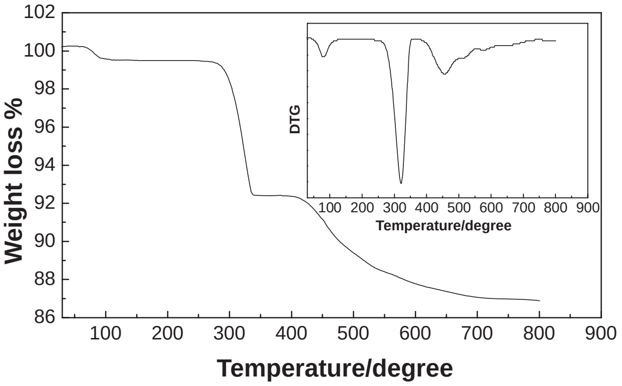

Figure 3. Thermogravimetry and differentiate thermogravimetry trace of the as-synthesized $Eu(OH)_3$ products.

transition mechanism, which indicates Eu^{3+} ions embedded in a site without inversion symmetry. However, the main emission peak of $Eu(OH)_3$ nanorod located at 591 nm (Supporting Information 2),[13] which is assigned to the $^5D_0$–$^7F_1$ magnetic dipole transition of Eu^{3+}. This difference can be explained assuming that Eu^{3+} ions occupy the center of inversion symmetry and that the $^5D_0$–$^7F_2$ transition is suppressed in hexagonal $Eu(OH)_3$ phase.[10]

Although the exact mechanism for the formation of these nanorods is still unclear, we believe that the growth of nanarods is not catalyst-assisted or template-directed one. Because the only starting material used in our synthesis is pure rare RE oxide, it is likely that the growth is governed by a solid solution process, in which the oxide molecules dissolved and hydroxylated from the source oxide under hydrothermal treatment, subsequently to recrystallize and grow into nanorods through a dissolution–recrystallization process.[11] It is obvious that bulk particles are the precursors for further crystal growth rather than ionic species, an important difference to previous reports arises from a homogeneous nucleation and solution growth process.[12]

In summary, we have found a simple method to prepare $Eu(OH)_3$ and Eu_2O_3 nanorods by facile hydrothermal treatment. Such nanorods have a variety of promising applications. The simplicity of hydrothermal process, cheapness, and availability of raw materials are advantages favoring the scaling-up of nanorods. RE oxide nanorods could be doped with different RE elements and used for fabricating nanosize optical devices based on the characteristics of individual nanorods. We believe that, these nanorod structures will find applications in optoelectronic and nanoscale devices, low-dimensional physics and material scence, and biological technology. Further work is under way to study the formation mechanism and controllable probability by changing the temperature, time and the concentration of NaOH solution.

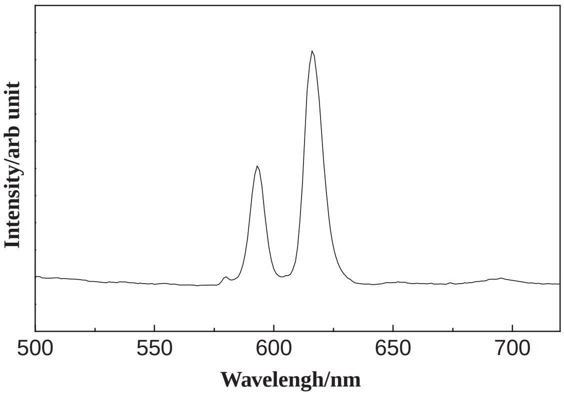

Figure 4. Luminescence spectrum of Eu_2O_3 nanorod at room temperature (excited at 396 nm).

The authors thank the financial support from the National Natural Science Foundation (No. 20376009) of China.

References and Notes

1 S. Iijima, *Nature* **1991**, *354*, 56.
2 P. M. Ajayan, *Chem. Rev.* **1999**, *99*, 1787.
3 X. W. Ge, Y. H. Ni, Zh. Ch. Zhang, *Radiat. Phys. Chem.* **2002**, *64*, 223; V. G. Kumar, K. B. Kim, *Ultrason. Sonochem.* **2006**, *13*, 549; J. M. Kim, J. K. Park, K. N. Kim, Ch. H. Kim, H. G. Jang, *Curr. Appl. Phys.* **2006**, *6S1*, e198.
4 G. Y. Adachi, N. Imanaka, *Chem. Rev.* **1998**, *98*, 1479.
5 K. S. Sohn, W. Zeon, H. Chang, S. K. Lee, H. D. Park, *Chem. Mater.* **2002**, *14*, 2140; K. B. Kim, K. W. Koo, T. Y. Cho, H. G. Chun, *Mater. Chem. Phys.* **2003**, *80*, 682; Z. Wang, D. Yuan, D. Xu, M. Lu, X. Cheng, L. Pan, X. Shi, *J. Cryst. Growth* **2003**, *255*, 348.
6 H. Eilers, B. M. Tissue, *Chem. Phys. Lett.* **1996**, *251*, 74.
7 A. Patra, E. Sominska, S. Ramesh, Y. Koltypin, Z. Zhong, *J. Phys. Chem. B* **1999**, *103*, 3361.
8 G. Sh. Wu, L. Zhang, B. Ch. Cheng, T. Xie, X. Y. Yuan, *J. Am. Chem. Soc.* **2004**, *126*, 5976.
9 V. G. Pol, O. Palchik, A. Gedanken, I. Felner, *J. Phys. Chem. B* **2002**, *106*, 9737.
10 G. Wakefield, H. A. Keron, P. J. Dobson, and J. L. Hutchison, *J. Colloid Interface Sci.* **1999**, *215*, 179.
11 J. Lu, Y. Xie, F. Yu, L. Y. Zhu, *J. Mater. Chem.* **2002**, *12*, 2755.
12 B. Mayers, Y. N. Xia, *Adv. Mater.* **2002**, *14*, 279.
13 Supporting Information is available on the CSJ-Journal web site; http://www.csj.jp/journals/chem-lett/index.html.

Published on the web (Advance View) February 24, 2007; doi:10.1246/cl.2007.468